

# Broken rotor bar diagnosis in induction machines through stationary wavelet packet transform and multiclass wavelet SVM

Hassen Keskes<sup>a</sup>, Ahmed Braham<sup>a,b,\*</sup>, Zied Lachiri<sup>b,c</sup>

<sup>a</sup> Research Laboratory, Matériaux, Mesures et Applications (MMA), INSAT, Tunisia

<sup>b</sup> Institut National des Sciences Appliquées et de Technologie (INSAT), Carthage University, Tunisia

<sup>c</sup> Research Laboratory, LR-SITI, Ecole National d'Ingénieurs de Tunis (ENIT), Tunisia

## ARTICLE INFO

### Article history:

Received 24 May 2012

Received in revised form

24 September 2012

Accepted 19 December 2012

Available online 30 January 2013

### Keywords:

Broken rotor bar

Fault diagnosis

Stationary wavelet packet transform

Multiclass SVM

Wavelet kernel

## ABSTRACT

This paper presents the establishing of intelligent system for broken-rotor-bar (BRB) diagnosis based on a novel combination of both, stationary wavelet packet transform (SWPT) and multiclass wavelet support vector machines (MWSVM). The SWPT is used for feature extraction under lower sampling rate. In fact, it is demonstrated through experimental results that the use of the lower sampling rate does not affect the performance of SWPT to detect BRB, while requiring much less computation and low cost implementation. The multiclass SVM (MSVM) is used to automatically recognize the faults. Different MSVM strategies are compared with various kernel functions in terms of classification accuracy, training and testing complexity. The classification results show that the wavelet kernel function detects the faulty conditions with a higher accuracy.

© 2013 Elsevier B.V. All rights reserved.

## 1. Introduction

Thanks to its robustness and the convenient power–weight ratio, the induction motor (IM) has dominated the field of electromechanical energy conversion. Nevertheless, in industrial application, IM is subject to unavoidable stress which creates failures in its different parts. Hence, condition monitoring has become necessary to predict the failure and the subsequent interruptions [1–5]. Despite its robustness, the IM presents some faults such as BRB [1–6]. This failure has become an important issue in the field of fault diagnosis. Indeed, operating IM with BRB may not only damage the motor itself, but can also have a catastrophic impact on the related machines [1–4]. The BRB introduces a distortion in the air-gap field that produces sideband component around the fundamental frequency in the current spectrum [4–7]. The frequency fault is given by:

$$f_b = (1 \pm 2s)f_s \quad (1)$$

where  $f_b$  is the sideband frequency associated to the BRB,  $s$  is the motor slip per unit and  $f_s$  is the fundamental frequency.

The motor current signature analysis (MCSA) is one of the most used techniques in fault detection analysis of IM [1–6]. The

main purpose of MCSA is to analyze the stator current and to detect the current harmonics related to the fault. The success of this technique lies on its simplicity and ability to detect all kind of defects: it only needs one current sensor and a straightforward signal processing technique [6–10]. Recently, the wavelet transform in its two variants, namely, discrete wavelet transform (DWT) [11–15] and wavelet packet transform (WPT) [16,17], has become one of the most widely used signal processing technique for IM diagnosis. Particularly, Sadeghian et al. [16] presented an algorithm for the online detection of BRB based on WPT with sampling frequency  $F_s = 1920$  Hz and number of samples  $N_s = 9984$ . The extracted features and the slip value are used by a neural network for faults classification. Furthermore, and in order to detect the same fault, Cusidó et al. [12] combined wavelet and power spectral density techniques to give the power detail density as a fault factor with  $F_s = 6$  kHz and  $N_s = 50,000$ . In [12,16], the experimental results showed that the proposed methods are able to detect the faulty conditions with high accuracy. However these techniques needed slip estimation which has made the automatic detection very difficult. To overcome this problem Kia et al. [11] applied the DWT to the space–vector magnitude of the stator phase current and computed the coefficient energy associated to the rotor fault with  $F_s = 10$  kHz and  $N_s = 65,536$  samples. This approach was successfully tested to IM under different BRB fault severities without slip estimation. Nevertheless, the use of the space–vector current requires three current sensors which made detection more expensive. Bouzida et al. [13] employed one current

\* Corresponding author. Tel.: +216 98 341415, fax: +216 71 704329.

E-mail addresses: [keskes.hassen@gmail.com](mailto:keskes.hassen@gmail.com) (H. Keskes), [ahmed.braham@insat.rnu.tn](mailto:ahmed.braham@insat.rnu.tn) (A. Braham), [zied.lachiri@enit.rnu.tn](mailto:zied.lachiri@enit.rnu.tn) (Z. Lachiri).

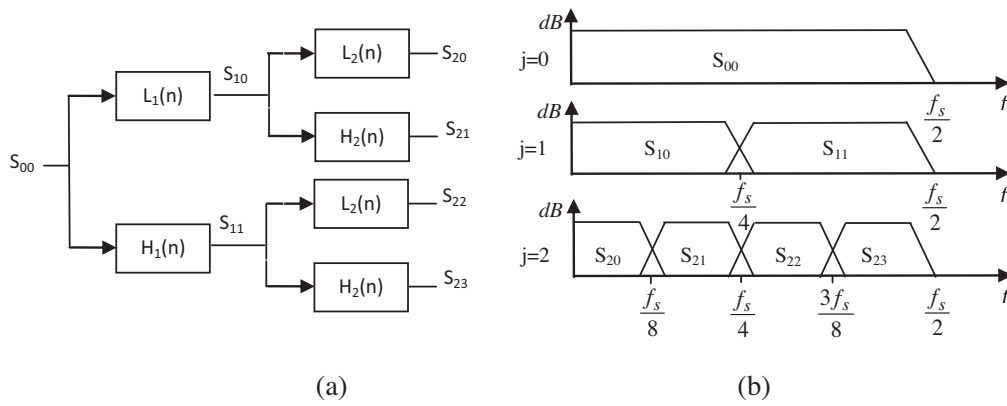


Fig. 1. SWPT: (a) structure decomposition and (b) coefficients frequency range.

sensor and DWT to detect BRB under non-stationary signals with  $F_s = 10$  kHz and  $N_s = 100,000$  samples. Yet, this method required good knowledge of the signals to find the correct  $F_s$ ,  $N_s$  and mother wavelet to improve the detection of faults. As a matter of fact, the sampling rate and number of samples are closely related to the fault detection performance. In addition, the implementation of condition monitoring system is often expensive. Therefore and in order to reduce the cost implementation it is worth mentioning that is necessary to select low sampling rate and a small number of samples while preserving fault detection performance [5].

In this work, it is demonstrated that lower sampling rate of  $F_s = 200$  Hz and a reduced number of samples,  $N_s = 1024$ , can be used for BRB detection.

Unlike previous works where either DWT or WPT is employed to diagnose BRB, in this paper, it is proven that using SWPT comes with great benefits. Indeed, DWT and WPT suffer from lack of shift invariance [18,19]. These shifts can lead to serious problems in the classification, identification, and faults detection [18,19]. The SWPT technique is designed to solve this problem by eliminating the down sampling at each level.

The SWPT is only used to extract the sensitive feature related to the fault but do not allow automatic fault detection. Nowadays, there is a demand to incorporate the learning techniques that can make decisions on the health of the machine automatically and reliably. SVM is relatively a new pattern recognition method based on statistical learning theory introduced by Vapnik [20]. It has been used in many fault diagnosis of IM with good performances [21–26]. The main idea behind SVM is to find the hyper-plane with maximum margin by separating the two-class samples. In the case where data is not linearly separable, SVM can map the input vector into a high dimensional space via a kernel function that satisfies the conditions of Mercer's theorem [27]. Kernel function plays an important role in SVM classification. Many kernel functions can be used: linear, polynomial (Poly), radial basis function (RBF), or sigmoid-shaped function. Recently, some wavelet kernel functions have been successfully applied in many fields of application like classification and nonlinear function estimation [28]. Although, SVM was originally designed to fulfill binary classification [20], several methods have been proposed to construct a MSVM. Among which two approaches are suggested in the literature: one against all (OAA) and one against one (OAO) [29,30]. These methods were mainly evaluated using classical kernel functions especially RBF and Poly [29,30]. Indeed, there is not a particular explanation concerning the use of wavelet kernel.

In this paper and in addition to using lower sampling rate and low number of samples the combination of SWPT and MSVM is

used for BRB fault detection. It is demonstrated that under such low sampling rate, DWT and WPT are not suitable for BRB detection. At the classification stage, the accuracy and complexity of both OAO and OAA strategies are compared using three kernel functions, namely RBF, Poly and wavelet.

The reminder of this paper is organized as follows: Section 2 recalls the DWT, WPT, and SWPT techniques. Section 3 introduces the fundamental of the wavelet kernel as well as MSVM. Section 4 describes the experimental setup and motor data specifications. Section 5 outlines the fault-detection schemes together with SWPT feature extraction. Finally, Section 6 summarizes the simulation results and observations. Section 7 concludes the findings of this paper.

## 2. Stationary wavelet packet transform

DWT is the first discrete implementation of wavelet transform [18,19], it consists on filtering the input signal by a low pass filter ( $L$ ) and high pass filter ( $H$ ) leading to two sub-bands called respectively approximations and details, followed by a decimation factor of both. In the next steps, the filter bank is successively applied only to the approximation coefficients. WPT is a generalization of DWT, where the filtering process is applied to decompose both approximations and details sub-bands while still decimating the filters outputs [18,19]. In the DWT and WPT, a fundamental computational step is down-sampling. On the contrary, the SWPT is implemented without down-sampling, keeping all the elements in the coefficients across all the decomposition levels [18,19]. The structure of a two level SWPT is shown in Fig. 1(a). Where  $S_{00}$  is the original signal, SWPT coefficients can be computed for each level  $j$  by:

$$S_{j+1,2n}(t) = \sqrt{2} \sum_K H_{j+1}(k) S_{j,n}(2t - k) \quad (2)$$

$$S_{j+1,2n+1}(t) = \sqrt{2} \sum_K L_{j+1}(k) S_{j,n}(2t - k) \quad (3)$$

where  $n$  is node number.

The SWPT coefficient frequency ranges are demonstrated in Fig. 1(b). At every level, the SWPT frequency resolution is:

$$f_r = \frac{f_s}{2^{j+1}} \quad (4)$$

The frequency bandwidth of SWPT coefficient is  $[nf_s/2^{j+1}, ((n+1)f_s)/2^{j+1}]$ .

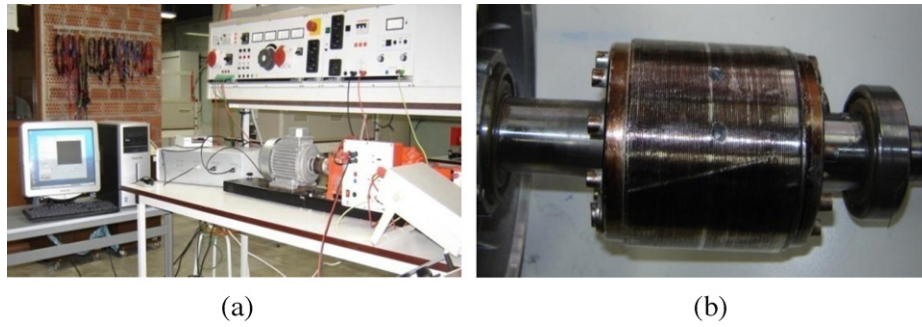


Fig. 2. The experimental setup (a) and rotor with two broken bars (b).

### 3. Multiclass wavelet SVM

In this section, the wavelet kernel, OAA and OAO MSVM strategies are presented.

#### 3.1. Wavelet kernel

The WSVM aims at finding the ideal classification in the space spanned by multidimensional wavelet. The concept behind the wavelet analysis is to express a signal by a family of functions generated by  $h(x)$  called mother wavelet [28]:

$$h_{a,c}(x) = |a|^{-1/2} h\left(\frac{x-c}{a}\right) \quad (5)$$

where  $x, a, c \in \mathbb{R}$ ,  $a$  is a dilation factor, and  $c$  is a translation factor.

A common multidimensional wavelet function can be expressed as the product of 1D wavelet function [28]:

$$h(x) = \prod_{i=1}^N h(x_i) \quad (6)$$

where  $N$  is the dimension number.

Let  $h(x)$  denotes a mother kernel function. Then dot-product wavelet kernels are [28]:

$$k(x, x') = \prod_{i=1}^N h\left(\frac{x_i - c_i}{a}\right) h\left(\frac{x'_i - c'_i}{a}\right) \quad (7)$$

The decision function for classification is [28]:

$$f(x) = \text{sign} \left( \sum_{i=1}^N \alpha_i y_i \prod_{j=1}^N h\left(\frac{x_i^j - x'_i^j}{a_i}\right) + b \right) \quad (8)$$

#### 3.2. Multiclass support vector machines

OAA is the simplest MSVM strategies. It involves  $k$  binary SVM classifiers, one for each class. Each binary SVM is trained to separate one class from the rest. The winning class is the one that corresponds to the SVM with highest output. This approach may suffer from error caused by markedly imbalanced training sets. The advantage of OAA is the fastness of classification, but its training is the most computationally expensive because each SVM is optimized on all the  $N$  training samples [29,30]. OAO involves  $k(k-1)/2$  binary SVM classifiers. Each classifier is trained to separate each pair of classes. There are different strategies used to combine these binary classifiers. The crucial widely used strategy is a majority voting. The class with the maximal number of votes is the result of classification. In this approach, more binary classifiers are used than in OAA, but the total classification performance can be efficiently improved efficiently [29].

### 4. Experimental setup and motor-data specifications

The prototype machine used in experimental setup has the following rated values: 0.55 kW (0.75HP), 380 V, 1.7 A, 1390 rpm, 50 Hz, IP 55, Class F and 4 poles. Fig. 2(a) shows the test bench of the IM. The data was acquired by using a current amplifier, based on three LEM current sensors, which amplify the IM stator currents before they are sent to the user interface Pentium PC. The motor was tested with a healthy and a faulty rotor that has one and two broken bars. BRB defects have been manually produced by drilling bar in the rotor cage, see Fig. 2(b). The needed load of the IM was established by connecting the test motor to a DC motor, which is capable to simulate any desired load condition. The load is varied from 0% to 100%, the corresponding slip is  $s_{\min} = 1.2\%$  to  $s_{\max} = 6.3\%$ . In the experiments, for each condition motor, healthy (HLT), 1BRB and 2BRB, 15 acquisitions have been done for five different load levels of the motor namely 0%, 25%, 50%, 75% and 100%, with  $F_s = 200$  Hz and  $N_s = 1024$  samples.

### 5. Fault detection scheme and feature extraction

The block diagram of a MSVM based on fault diagnosis is demonstrated in Fig. 3. The system consists of three sections: data acquisition, feature extraction, training and testing process. Therefore, the classification accuracy depends mainly on the quality of the feature extracted.

Measured values of the slip vary between 1.2% and 6.3%. Thus, the frequency bandwidth affected by the rotor fault is computed

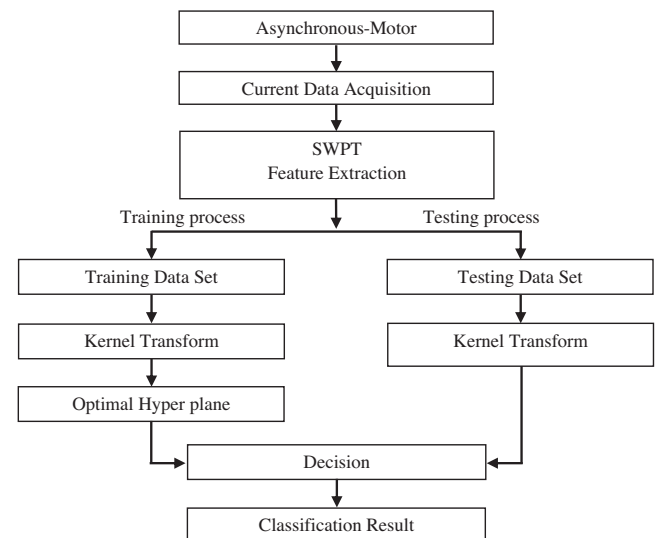


Fig. 3. Block diagram of a MSVM classifier system.

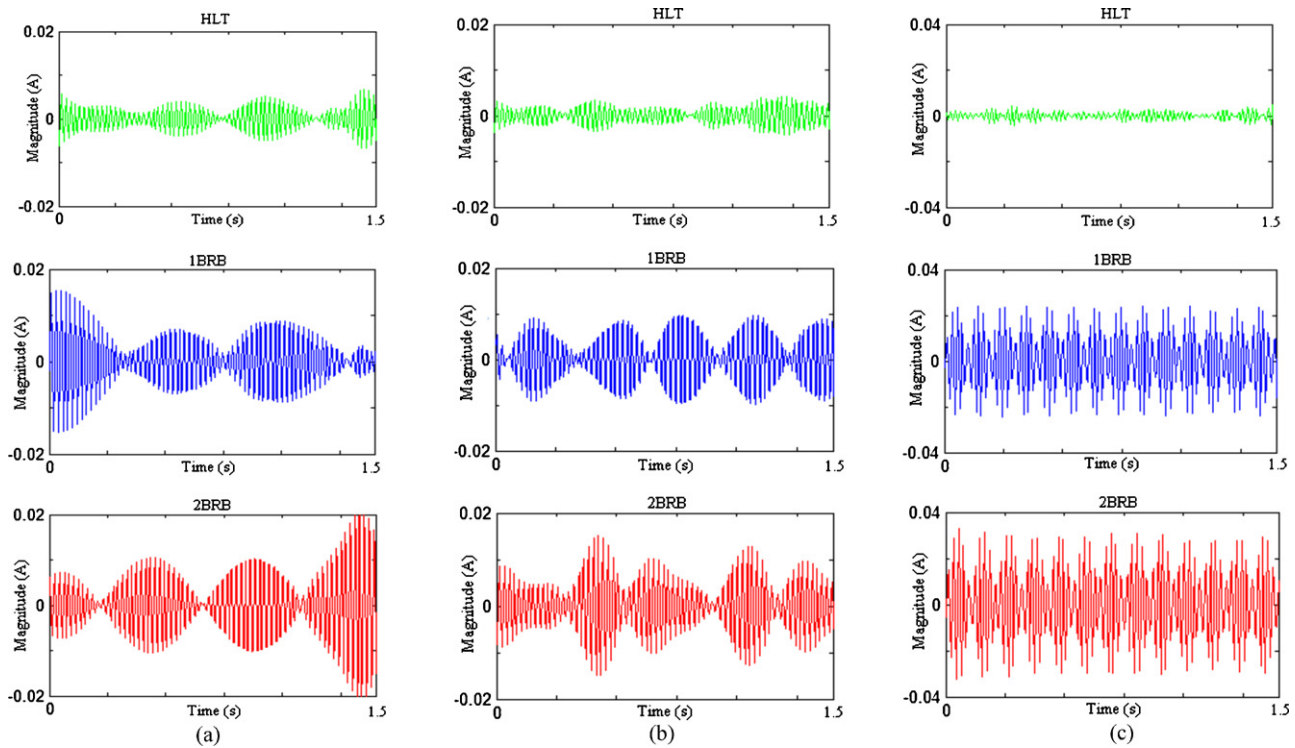


Fig. 4. Evolution of  $S_{7,63}$  (a),  $S_{6,31}$  (b) and  $S_{5,15}$  (c) for HLT, 1BRB and 2BRB motor conditions.

using (1) as [43.7, 48.8 Hz] for left sideband harmonic,  $f_1$ , and [51.2, 56.3 Hz] for the right sideband harmonics,  $f_2$ .

Using 200 Hz as a sampling rate, the DWT coefficients which cover the affected frequency bandwidth are  $C_{d1}$  [0.50 Hz],  $C_{d1}$  [50.100 Hz]; and  $C_{d2}$  [25.50 Hz]. The presence of fundamental frequency in all the coefficients makes DWT not suitable for BRB detection. Table 1 shows the SWPT and WPT coefficients which contain fault frequency bandwidth. It can be seen that the fundamental frequency is filtered which makes the coefficients very sensitive to the fault. However, in WPT the signal is down sampling at each level. At level 7, the length of signal will be  $1024/2^7 = 8$  samples so the WPT coefficients cannot detect BRB. Compared to WPT, SWPT has the best temporal resolution because it is implemented without down-sampling.

In SWPT the shape of the frequency response of the filters depends on the kind and the order of the mother wavelet used in the analysis. Some authors showed that all these types of mother wavelets gave similar results in motor diagnosis [13]. In this paper the orthogonal Daubechies at order 2 is used [18]. Fig. 4 shows the evolution of  $S_{7,63}$  at a load of 0% (a),  $S_{6,31}$  at a load of 25% (b) and  $S_{5,15}$  at a load of 75% (c) for a HLT, one and two BRB. It is observed that the selected coefficients for the healthy rotor situation are always very small, while for faulty conditions, the feature coefficients are changing with the load torque. It is worth pointing out that, at different load conditions, there is close relationship between the magnitude of the selected coefficients and the severity of the fault. The

magnitude of the coefficients for the 2BRB configuration is greater than those of 1BRB. These differences in the feature coefficients between HLT, 1BRB and 2BRB motor conditions show that they can be used for BRB detection.

## 6. Results and discussions

As all pattern recognition methods, SVM approach is done through two phases: training and testing (Fig. 3), 2/3 of the samples, present the training data set. The rest is used for testing the classifier's generalization ability. For every sample, the energy of the selected SWPT coefficients is calculated to the build input vector for the related classifier. The MWSVM classification is done with SVM-KM Toolbox for Matlab [31]. In this paper, five kernel functions are used: RBF, Poly, wavelet Haar, wavelet Daubechies (Daub) and wavelet Symmlet (Symm). Inappropriate selection of kernel functions parameters leads to a decrease in the classification accuracy. The cross-validation method is used for kernel parameters selection. Table 2 presents the searching interval of every kernel parameter where  $\gamma$  is the kernel width,  $D$  is the degree of the polynomial,  $V$  is the number of vanishing moments,  $P$  is the number of points in the wavelet,  $j_{\max}$ ,  $j_{\min}$  are the maximal and minimal resolution and  $C$  is the penalty term. The MSVM is trained with optimum parameters.

Table 1  
Selected SWPT coefficients.

Frequency of BRB	SWPT coefficients	Frequency bandwidth (Hz)	Slip bandwidth	Load variation
Left sideband harmonic	$S_{5,15}$	[43.7; 46.8]	[3.2%; 6.3%]	[44%; 100%]
	$S_{6,31}$	[46.8; 48.4]	[1.6%; 3.2%]	[22%; 44%]
	$S_{7,63}$	[48.4; 49.2]	[1.2%; 1.6%]	[0%; 22%]
Right sideband harmonic	$S_{5,18}$	[53.2; 56.3]	[3.2%; 6.3%]	[44%; 100]
	$S_{6,34}$	[51.6; 53.2]	[1.6%; 3.2%]	[22%; 44%]
	$S_{7,66}$	[50.8; 51.6]	[1.2%; 1.6%]	[0%; 22%]



**Table 2**  
The kernel functions parameters.

Kernel functions	Parameters	The range of variation parameters
Rbf	C: penalty term	1–1000
Poly	$\gamma$ : The kernel width	0.1–10
	D: is the degree of the Polynomial	1–10
Haar	V: number of vanishing moments	1–6
Daub	P: number of points in the wavelet	4–8
Symm	$j_{\max}$ : maximal resolution	–10 to 6
	$j_{\min}$ : minimal resolution	–10 to 6
	C: penalty term	1–1000

Table 3 shows the kernel parameters, the strategy of MSVM, two types of correct classification rate for training and testing (CCR1 and CCR2), number of support vector, training and testing time. The rate CCR1 and CCR2, are mathematically expressed as

$$CCR1 = 1 - \frac{T1}{\text{Data total number}} \quad (9)$$

$$CCR2 = 1 - \frac{T1 + T2}{\text{Data total number}} = CCR1 - \frac{T2}{\text{Data total number}} \quad (10)$$

where T1 and T2 represent two types of error in the classification rate. T1 (type I) will correspond to the number of the confusion output classifier between healthy and faulty (one or two BRB). T2 (type II) will correspond to the classifier output number of one broken bar which is labeled as two broken bars. CCR1 gives information about SVM capacity to detect faulty or healthy motor without fault severity determination. CCR2 identifies the faulty motor and the number of BRB. The classification rate CCR1 is ranged from 98% to 100% for the training rate and 95–100% for the testing rate. It can be concluded that the classifiers detect the fault very well. In the rest of paper different SVM structures will be compared to have the best CCR2.

### 6.1. Kernel functions comparison

As it is shown in Table 3, SVM has high generalization ability, the training CCR2s vary between 95% and 100%. The bar chart depicted in Fig. 5 presents the testing CCR2s of all kernel functions under OAO and OAA. This graph shows that for OAO the Daub wavelet kernel is more efficient in the BRB fault detection and which is expressed

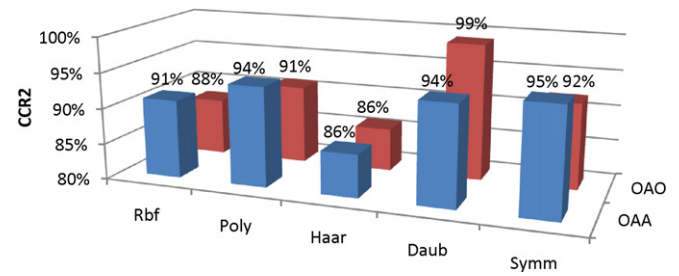


**Fig. 5.** OAA and OAO testing CCR2.

mathematically as:

$$CCR2_{OAO\_Daub} > CCR2_{OAO\_Symm} > CCR2_{OAO\_Poly} > CCR2_{OAO\_RBF} > CCR2_{OAO\_Haar} \quad (11)$$

For OAA, Symm wavelet kernel is the best kernel function:

$$CCR2_{OAA\_Symm} > CCR2_{OAA\_Daub} = CCR2_{OAA\_Poly} > CCR2_{OAA\_RBF} > CCR2_{OAA\_Haar} \quad (12)$$

However, comparing RBF and Poly with wavelet kernel training and testing times, this latter is relatively long. The order of training (TT) and testing (TST) time is:

$$TT_{Symm} > TT_{Daub} > TT_{Haar} > TT_{RBF} > TT_{Poly} \quad (13)$$

$$TST_{Symm} > TST_{Daub} > TST_{Haar} > TST_{RBF} > TST_{Poly} \quad (14)$$

The order is the same for both OAO and OAA strategies. As a result, the wavelet kernel classification process is more expensive in time than RBF and Poly.

### 6.2. Multiclass SVM strategies comparison

In [29], authors support that OAO is more accurate and less complex than OAA. The experimental results confirm the accuracy hypothesis. OAO gives the best testing CCR2 (99%). However in terms of complexity, it can be seen in Fig. 6(a) that under wavelet kernel, OAO have more complicated training process than OAA. In this section, we try to explain these results and compare OAA and OAO in terms of complexity.

#### 6.2.1. Training complexity

OAO and OAA theory is based on solving several binary classifications. To solve  $k$  class problem using OAO,  $k(k-1)/2$  binary SVM classifiers have been developed, and the samples number in each

**Table 3**  
Fault classification results.

Kernel parameters		Multiclass approach	Classification rate (%)				Nb of SVs	Training time (s)	Testing time (s)
			Training		Testing				
			CCR1 (%)	CCR2 (%)	CCR1 (%)	CCR2 (%)			
Rbf ( $\gamma$ , C)	(2, 1)	OA0	98	95	98	88	1100	0.2	0.014
	(2, 300)	OAA	100	100	100	91	318	0.3	0.011
Poly (D, C)	(2, 2)	OA0	99	95	100	91	168	0.1	0.003
	(2,100)	OAA	100	100	100	94	70	0.2	0.001
Haar (V, P, $j_{\max}$ , $j_{\min}$ , C)	(4, 4, −10, 0)	OA0	98	95	95	86	644	6	5.6
	(4, 4, −10, 0)	OAA	100	100	96	86	208	1.6	1.2
Daub (V, P, $j_{\max}$ , $j_{\min}$ , C)	(8, 4, −6, −10)	OA0	100	100	100	99	292	7.8	8.9
	(4, 4, −8, 0)	OAA	100	100	98	94	259	1.7	1.37
Symm (V, P, $j_{\max}$ , $j_{\min}$ , C)	(8, 4, −8, 0)	OA0	100	100	98	92	359	14	21
	(2, 4, −10, 0)	OAA	100	100	100	95	298	2.1	1.5

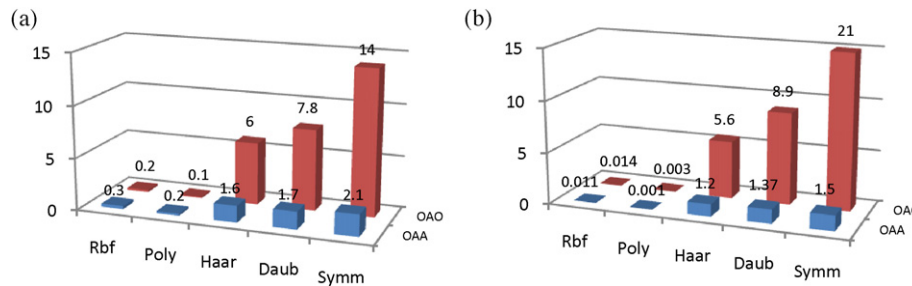


Fig. 6. OAA and OAO training time (a) and testing time (b).

**Table 4**  
OAA and OAO training time of binary class.

Kernel functions	RBF	Poly	Haar	Daub	Symm
$TT_{\text{of binary classifier OAO}}(s)$	0.003	0.001	0.057	0.074	0.102
$TT_{\text{of binary classifier OAA}}(s)$	0.025	0.016	0.107	0.113	0.14
$R$	0.8	0.4	3.7	4.6	5.1

classifier is  $n/k$ ,  $n$  is the total number of training data set. Whereas, OAA constructs  $k$  binary class with  $n$  samples for each classifier. The training time is expressed as:

$$TT \approx \text{number of binary classifier} \times TT_{\text{of binary classifier}} \quad (15)$$

$R$  is a comparison ratio of OAA and OAO training time:

$$R = \frac{TT_{\text{OAO}}}{TT_{\text{OAA}}} \approx \frac{nb_{\text{cOAO}} \times TT_{\text{of binary classifier OAO}}}{nb_{\text{cOAA}} \times TT_{\text{of binary classifier OAA}}}$$

$$R = \frac{TT_{\text{OAO}}}{TT_{\text{OAA}}} \approx \frac{(k(k-1)/2) \times TT_{\text{of binary classifier OAO}}}{k \times TT_{\text{of binary classifier OAA}}} \quad (16)$$

$$R = \frac{TT_{\text{OAO}}}{TT_{\text{OAA}}} \approx \frac{(k-1) \times TT_{\text{of binary classifier OAO}}}{2 \times TT_{\text{of binary classifier OAA}}}$$

Table 4 shows the  $TT$  of binary class under RBF, Poly, Haar, Daub and Symm. It is noticed that under RBF and Poly kernel,

$$R < 1 \quad \text{so} \quad TT_{\text{OAO}} > TT_{\text{OAA}} \quad (17)$$

While under wavelet kernel,

$$R > 1 \quad \text{so} \quad TT_{\text{OAO}} < TT_{\text{OAA}} \quad (18)$$

These results assert and explain the training time value shown in bar chart, Fig. 6(a).

### 6.2.2. Testing complexity

The decision function of binary class for SVM is

$$f(x) = \sum_{i=1}^N W_i \phi(x, x_i) + b \quad (19)$$

where  $N$  being the number of support vector (SV).

Obviously, the computation time of this decision function is proportional to the number of SV. In addition, for OAO it is necessary to evaluate  $k(k-1)/2$  decision functions and for OAA it is only  $k$ . As it is shown in Table 3, the OAO uses more SV than the OAA. Fig. 6(b) shows that the testing in OAA is faster than in OAO under all kernel functions. It can be concluded that the decision-making with the OAO strategy is more complex than with the OAA.

## 7. Conclusion

In this paper, a new method to detect BRB in IM using a combination of SWPT feature extraction and MWSVM is developed. In spite the fact that the diagnosis is realized under lower sampling rate, the SWPT presents a good feature extraction performance.

It is important to emphasize that feature extraction is done with only 6 features. Particularly in this study, OAO and OAA decomposition strategies are compared in terms of classification accuracy, training and testing complexity. Daubechies wavelet function combined with OAO give the best classification accuracy, 99%. In terms of training and testing process, OAA is about 5 times faster than OAO and required less number of SV. According to this result, SWPT and MWSVM can serve as a promising alternative for intelligent faults diagnosis in the future. Furthermore, the use of a lower sampling rate is a solid argument to implement this methodology in an embedded system.

## References

- [1] W.T. Thomson, M. Fenger, Current signature analysis to detect induction motor faults, *IEEE Transactions on Industry Applications* 7 (4) (2001) 26–34.
- [2] G.K. Singh, S. Ahmed Saleh Al Kazzaz, Induction machine drive condition monitoring and diagnostic research—a survey, *Electric Power Systems Research* 64 (2) (2003) 145–158.
- [3] M.E.H. Benbouzid, G.B. Kliman, What stator current processing-based technique to use for induction motor faults diagnosis? *IEEE Transactions on Energy Conversion* 18 (2) (2003) 238–244.
- [4] S. Nandi, H.A. Toliyat, X. Li, Condition monitoring and fault diagnosis of electrical motors—a review, *IEEE Transactions on Energy Conversion* 20 (4) (2005) 719–729.
- [5] B. Ayhan, H.J. Trussell, M.Y. Chow, M.H. Song, On the use of a lower sampling rate for broken rotor bar detection with DTFT and AR-based spectrum methods, *IEEE Transactions on Industrial Electronics* 55 (3) (2008) 1421–1434.
- [6] A. Braham, Z. Lachiri, Diagnosis of broken bar fault in induction machines using advanced digital signal processing, *International Review of Electrical Engineering* 5 (4) (2010) 1460–1468.
- [7] J.J. Rangel-Magdaleno, R.J. Romero-Troncoso, R.A. Osornio-Rios, E. Cabal-Yepez, L.M. Contreras-Medina, Novel methodology for online half-broken-bar detection on induction motors, *IEEE Transactions on Instrumentation and Measurement* 58 (5) (2009) 1690–1698.
- [8] M. Riera-Guaspa, J. Antonino-Daviu, J. Rusek, J. Roger-Folch, Diagnosis of rotor asymmetries in induction motors based on the transient extraction of faults components using filtering techniques, *Electric Power Systems Research* 79 (8) (2009) 1181–1191.
- [9] J. Pons-Llinares, J. Antonino-Daviu, M. Riera-Guaspa, M. Pineda-Sanchez, V. Climente-Alarcon, Induction motor diagnosis based on a transient current analytic wavelet transform via frequency B-splines, *IEEE Transactions on Industrial Electronics* 58 (5) (2011) 1530–1544.
- [10] T. Boukara, A. Lebaroud, A. Medued, Wavelet network for classification of induction machine faults using optimal time–frequency representation, in: *Proceedings of the 7th International Conference on Electrical and Electronics Engineering ELECO'11, Turkey*, 2011.
- [11] S.H. Kia, H. Henao, G.A. Capolino, Diagnosis of broken-bar fault in induction machines using discrete wavelet transform without slip estimation, *IEEE Transactions on Industry Applications* 45 (4) (2009) 1395–1404.
- [12] J. Cusidó, L. Romeral, J.A. Ortega, A. Garcia, J.R. Riba, Wavelet and PDD as fault detection techniques, *Electric Power Systems Research* 80 (8) (2010) 915–924.
- [13] A. Bouzida, O. Touhami, R. Ibtouen, A. Belouchrani, M. Fadel, A. Rezzoug, Fault diagnosis in industrial induction machines through discrete wavelet transform, *IEEE Transactions on Industrial Electronics* 58 (9) (2011) 4385–4395.
- [14] R. Kechida, A. Menacer, DWT wavelet transform for the rotor bar detection in induction motor, in: *Proceedings of the 2nd International Conference on Electric Power and Energy Conversion Systems EPECS, United Arab Emirates*, 2011.
- [15] J.R. Millan-Almaraz, R.J. Romero-Troncoso, A. Garcia-Perez, R.A. Osornio-Rios, Wavelet based methodology for broken bar detection in induction motors with variable speed drive, *Electric Power Components and Systems* 39 (3) (2011) 271–287.
- [16] A. Sadeghian, Ye Zhongming, W. Bin, Online detection of broken rotor bars in induction motors by wavelet packet decomposition and artificial neural

- networks, *IEEE Transactions on Instrumentation and Measurement* 58 (7) (2009) 2253–2263.
- [17] G.F. Bin, J.J. Gao, X.J. Li, B.S. Dhillon, Early fault diagnosis of rotating machinery based on wavelet packets—empirical mode decomposition feature extraction and neural network, *Mechanical Systems and Signal Processing* 27 (2012) 696–711.
- [18] S. Mallat, *A Wavelet Tour of Signal Processing. The Sparse Way*, Academic Press, United States, 2009.
- [19] C.S. Burrus, A.R. Gopinath, H. Guo, *Introduction to Wavelets and Wavelet Transforms: A Primer*, Prentice Hall, United States, 1997.
- [20] V. Vapnik, *Statistical Learning Theory*, Wiley, New York, 1998.
- [21] A. Widodo, B.S. Yang, Support vector machine in machine condition monitoring and fault diagnosis, *Mechanical Systems and Signal Processing* 21 (1) (2007) 2560–2574.
- [22] Y. Shengfa, C. Fulei, Fault diagnosis based on support vector machines with parameter optimisation by artificial immunisation algorithm, *Mechanical Systems and Signal Processing* 21 (3) (2007) 1318–1330.
- [23] A. Widodo, E.Y. Kim, S. Jong-Duk, B.S. Yang, C.C.T. Andy, G. Dong-Sik, C. Byeong-Keun, M. Joseph, Fault diagnosis of low speed bearing based on relevance vector machine and support vector machine, *Expert Systems with Applications* 36 (3) (2009) 7252–7261.
- [24] A. Braham, H. Keskes, Z. Lachiri, Multiclass support vector machines for diagnosis of broken rotor bar faults using advanced spectral descriptors, *International Review of Electrical Engineering* 5 (5) (2010) 2095–2105.
- [25] A. Ilhan, K. Mehmet, A. Erhan, A multi-objective artificial immune algorithm for parameter optimization in support vector machine, *Applied Soft Computing* 11 (1) (2011) 120–129.
- [26] D. Matic, F. Kulic, M. Pineda-Sanchez, I. Kamenko, Support vector machine classifier for diagnosis in electrical machines, application to broken bar, *Expert Systems with Applications* 39 (10) (2012) 8681–8689.
- [27] C.J.C. Burges, Geometry and invariance in kernel based methods, in: B. Schölkopf, C.J.C. Burges, A. Smola (Eds.), *Advances in Kernel Methods – Support Vector Learning*, MIT Press, Cambridge, USA, 1999, pp. 89–116.
- [28] L. Zhang, W. Zhou, L. Jiao, Wavelet support vector machine, *IEEE Systems, Man, and Cybernetics Society* 34 (1) (2004) 34–39.
- [29] C. Hsu, C. Lin, A comparison of methods for multiclass support vector machines, *IEEE Transactions on Neural Networks* 13 (2) (2002) 415–425.
- [30] R. Rifkin, A. Klautau, In defense of one-vs-all classification, *Journal of Machine Learning* 5 (2004) 101–141.
- [31] S. Canu, Y. Grandvalet, V. Guigue, A. Rakotomamonjy, *SVM and Kernel Methods Matlab Toolbox, Perception Systèmes et Information*, INSA de Rouen, France, 2008.